COMSOL
CONFERENCE
2023 MUNICH

Simulation of Sheet Molding during Through Air Drying of Tissue Paper within a Papermaking Framework

K. Rezk[1], B. Sjöstrand[1]
1. Pro2BE, the research environment for Processes and products for a circular forest-based bioeconomy, Department of engineering and chemical sciences, Karlstad University, Karlstad, Sweden

Abstract
A way to improve product performance of tissue grade paper products is to replace the press section with a Through Air Drying (TAD) section which is a technique where paper sheets are moulded into a structured fabric by vacuum boxes and transferred over one or more TAD cylinders with steam heated displacement drying. The process of sheet molding is modelled with Comsol Multiphysics where the computational model is setup with a 2-dimensional representation of the paper sheet. The tissue sample with randomly distributed fibre positions is generated using a MATLAB script written in the *Livelink* interface with Comsol. The process is simulated with the *Moisture Flow* multiphysics interface. The comprising physical modules are the *Laminar Flow* and the *Moisture Transport in Air* modules. Respectively, these modules calculate the velocity and pressure field of the moist air as well as the relative humidity, which is a rewrite of the concentration of water in air. The fibres in the sheet are modelled as porous media where the fibres contain both moist air and liquid water in equilibrium. In this paper, a basis weight at roughly 20 g/m^2 is simulated and compared to laboratory data. The aim of the model is to estimate solid content in the paper sheet over vacuum time as well as energy demand and required airflow through the structure.

Keywords: CFD, Dewatering, Moisture transport, tissue paper, through air dying.

Introduction
Water removal during paper and board manufacturing is an energy intensive process. The dewatering process in paper and board manufacturing generally consists of four stages with progressively high energy demand [1, 2]. The first stage comprises water removal with gravity or centrifugal forces where water escapes without additional energy input and then with help of static elements in the geometry of the paper machine, followed by low and high vacuum pressure. In the second stage of vacuum exposure, where higher levels of vacuum pressure are applied through suction boxes [2-8]. Most of the suspended water is removed during gravitational and vacuum dewatering [9]. The third stage is performed in the press section by compressing the paper in one or more press nips [10]. The last stage, which far exceeds the other stages in energy demand, is comprised by thermal drying where remaining water in fibres are evaporated on steam-heated cylinders [9, 11]. Hence, improving the mechanical dewatering processes prior to the thermal stage could reduce major production cost.

A number of researchers have studied vacuum dewatering experimentally using laboratory equipment as well using pilot scale machines [2-8, 12-21]. Process parameters that influence sheet dryness such as applied vacuum, dwell time and basis weight have been analysed.[4, 6, 13, 22-25] These studies show that a prolonged dwell time would increase dryness to a certain level. To reach a higher dryness level, increased vacuum pressure is necessary.

Numerous researchers have conducted theoretical and numerical analysis on various aspects on vacuum dewatering such as single-flow mechanics in fibrous porous media where permeation through compressible fiber beds, permeability in various representative fiber structures were studied as well as penetrated air volume calculated and compared to experimental data [26-30]. Some attempts on simulating the two-phase flow behavior during the early stage of dewatering of the unbound water where progression on estimating the dwell time and dry content with varying pressure pulses has been conducted in [16, 31, 32]. While there are improvements that need to me made on the estimation of the dewatering rate, the penetrated air volume showed excellent agreement with experimental data.

Fluid inertia as well as spatial heterogeneity has been studied for moderate Reynolds number in various fiber arrangements by [33-37]. Moreover, the influence on the permeability based on sample size, boundary conditions, homogeneity and isotropy were studied. The relations are used to predict permeability for various fiber arrangements and porosity levels.

A way to improve product performance of tissue grade paper products is to replace the press section with a Through Air Drying (TAD) section which is a technique where paper sheets are moulded into a structured fabric by vacuum boxes and transferred over one or more TAD cylinders with steam heated displacement drying (Tysén 2018, Tysén et al. 2015; 2018). Much like conventional papermaking machines, where the Yankee cylinder is the most energy requiring step, the TAD cylinders have by far the highest energy demand. Hence, improving the drying rate in the molding process is necessary from an energy demand standpoint. The process of sheet molding is modelled with Comsol Multiphysics where the computational model is setup with a 2-dimensional representation of the paper sheet. The tissue sample with randomly distributed fibre positions is generated using a MATLAB script written in the *Livelink* interface with Comsol. The process is simulated with the *Moisture Flow* multiphysics interface. The comprising physical modules are the *Laminar Flow* and the *Moisture Transport in Air* modules. The purpose of this paper is to gain a better understanding of driving as well as limiting mechanisms of moisture transport in porous media concept of TAD molding system. The aim is to develop a first draft of a computational model that can simulate the change in solid content

Theory / Numerical Set Up

Wood fibres for papermaking and paper sheets are both hygroscopic materials and, as such, contain bound water within the sheet network structure and within fibre walls. The network of fibres in a sheet as well as the fibres themselves can be viewed as porous media and understanding the physics and characteristics of fluid transport is key in numerically assessing water removal rate. Physical effects such as fluid flow and transport of fluids in different phases is considered. Heat transfer is excluded from these simulations at this stage as evaporative cooling is assumed to have neglectable effects on the drying process.

Computational domain

The computational model is setup with a 2-dimensional representation of the paper sheet. The tissue sample with randomly distributed fibre positions is generated using a MATLAB script written in the *Livelink* interface with Comsol. The script creates fibres and randomly position them throughout the domain, which represents the paper, see Fig. 1. The code can be set to create fibres comprising of various basis weights and paper sheet porosities. In this paper, a sheet comprising of a basis weight at 18 g/m^2 and a porosity at approximately 0.7 were simulated and analysed. Ten different structures were created in the Livelink Matlab script.

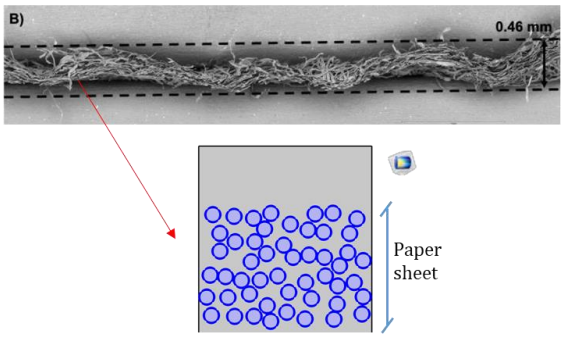

Figure 1. 2-dimensional representation of paper sheet model in Comsol. The upper SEM image is from the study [20].

The basis weight (g/m^2) is a standard measurement in paper manufacturing and it represent the weight of the paper in relation to a standard size. More specifically, it is the ratio between the mass of dry substance and the surface area of the sample.

$$BW = \frac{N\rho_L}{S} \qquad (1)$$

Where ρ_L coarseness or length density (kg/m) of a fibre, N is the number of fibres, whereas S (m) is the height of the sample.

Modelling continua in porous media

Porous materials such as networks of wood fibres has a complex solid structure and is highly discontinues from a continuum theory perspective, see Fig. (2). This is resolved by viewing the modelled structure as a porous media in several layers, that is, the wood fibres are interpreted as a mixture of different materials (solids and fluids) with measurable quantities in a macroscopic field.

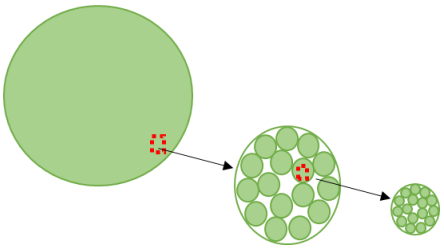

Figure 2. A 2-dimensional schematic representation of the structure of a single wood fibre and, on smaller scales, bundles of microfibrils.

Governing Equations / Numerical Model

At the start of the simulation process, the fibres are saturated with water, although surrounded by moist air. As air flows through the paper sheet, the fibres are dried due to moisture mitigation from the core of the fibre to the surface through convection and capillary forces. At the surface, water is evaporated though forced convection and vapour diffusion. The process is simulated with the *Moisture Flow* Multiphysics interface. The comprising physical modules are the *Laminar Flow* and the *Moisture Transport in Air* modules.

Pore space in the paper model

The penetrating airflow is modelled with the continuity and Navier stokes equations in COMSOL Multiphysics 6.1, see Eqs. (2) and (3),

$$\frac{\partial \rho}{\partial t} + \frac{\partial (\rho u_i)}{\partial x_i} = 0 \quad (2)$$

$$\frac{\partial (\rho u_i)}{\partial t} + \rho u_j \frac{\partial u_i}{\partial x_j} = -\frac{\partial p}{\partial x_i} + \frac{\partial}{\partial x_j}\tau_{ij} - \rho g_i \quad (3)$$

where τ_{ij} is the deviatoric stress tensor which includes the bulk viscosity due to compressibility in the air, see Eq. (4).

$$\tau_{ij} = \mu\left(\frac{\partial u_i}{\partial x_j} + \frac{\partial u_j}{\partial x_i} - \frac{2}{3}\mu\frac{\partial u_k}{\partial x_k}\delta_{ij}\right) \quad (4)$$

Turbulence modelling was excluded from the simulations due to small length scales in the order of 10e^{-6} m and, hence, leading to low Reynolds numbers.

The moisture transport in the air is described with a modified advection diffusion model shown in Eq. (5),

$$M_v\frac{\partial c}{\partial t} + M_v u_j \frac{\partial c}{\partial x_j} - M_v D_v \frac{\partial^2 c}{\partial x_j^2} = G \quad (5)$$

where M_v (kg/mol) is the molar mass of water vapour, D_v (m^2/s) is the vapor diffusion in air coefficient and G (kg/m^{3}s) is the moisture source or sink term. The concertation term in in Eq. (5) is related to the relative humidity with the vapor saturation concentration.

$$c = \varphi_v c_{sat} \quad (6)$$

Porous media modelling in wood fibre

The wood fibres are typically hygroscopic materials and, as such, should be modelled as a porous media. The fibres contain two phases in equilibrium, which is the liquid water and the moist air. The driving force for transportation of each phase is vapor diffusion and convection in air, as well as capillary flow and convection for water. Assuming that the inertial forces in the fibres are neglectable, Darcy's correction model is used to relate pressure gradients to the volume averaged superficial velocity

$$\langle u_i \rangle = -\frac{\kappa_{ij}}{\mu}\frac{\partial p}{\partial x_i} \quad (7)$$

where κ_{ij} (m^2) is permeability coefficient and μ (Pa·s) is the dynamic viscosity. The permeability is typically decomposed into intrinsic permeability and relative permeability for multiphase flow in porous media according to [38]. The intrinsic parameter represents the permeability of liquid or gas in an entirely saturated state, i.e. the pores in the fibre contain the maximum amount of water. The relative permeability varies between zero and one for each phase depending on the water content within the fibre walls. The total permeability is, hence, the product of the intrinsic and relative permeability.

$$\begin{cases} k_g = k_{gi}k_{gr} \\ k_w = k_{wi}k_{wr} \end{cases} \quad (8)$$

The equations that describe the relative permeability for each phase are described in Eq. (9) and (10). [38]

$$\begin{cases} k_{gr} = 1 - 1.1S_w, if\ S_w < \frac{1}{1.1} \\ k_{gr} = 0 \quad\quad\quad\quad , if\ S_w > \frac{1}{1.1} \end{cases} \quad (9)$$

$$\begin{cases} k_{wr} = \left(\frac{S_w - S_{ir}}{1 - S_{ir}}\right)^3, if\ S_w > S_{ir} \\ k_{wr} = 0 \quad\quad\quad\quad , if\ S_w < S_{ir} \end{cases} \quad (10)$$

The intrinsic permeability for wood fibres are used from [38].

Fluid transport in and between wood fibres is described with the following equation

$$\frac{\partial W(\varphi_v)}{\partial t} + \rho_g u_{g,j}\frac{\partial \omega_v}{\partial x_j} + \frac{\partial g_w}{\partial x_j} + \rho_g u_{l,j}\frac{\partial \rho_l}{\partial x_j} + \frac{\partial g_{lc}}{\partial x_j} = G \quad (11)$$

where g_w (kg/(m·s)), see Eq. (12), is the vapor transport in the gaseous phase in the wood fibre. As the Millington and Quirk equation is used calculate the effective diffusivity in see Eq. (12). The capillary flux term g_{lc} (kg/(m·s)), see Eq. (13), is described as the relative humidity gradient of the moisture content and an added diffusivity term D_w (m^2/s), see Eq. (14). [38] The moisture content, $W(\varphi_v)$, is a function of the relative humidity, see Eq. (15).

$$g_w = -\rho_g D_{eff}\frac{\partial \omega_v}{\partial x_j} \quad (12)$$

$$g_{lc} = -D_w\frac{\partial W(\varphi_v)}{\partial \varphi_v}\cdot\frac{\partial \varphi_v}{\partial x_j} \quad (13)$$

$$D_w = 1\cdot 10^{-8}e^{\left(-2.8 + \frac{2w(\varphi_v)}{(1-\varepsilon_p)\rho_f}\right)} \quad (14)$$

$$W(\varphi_v) = \varepsilon_p\left(\rho_l s_l + \rho_g\omega_g(1 - s_l)\right) \quad (15)$$

The liquid saturation, s_l, is a dimensionless parameter and it describes the amount of water left within the pores, ε_p is the porosity of the wood fibres and ω_g is vapour mass fraction.

Model simplifications

Some of the major assumptions this model relies on is:

- Aligned fibre positions due to 2-dimensional representation of the paper sheet

- The forming and deformation of the fibre web during the TAD molding process is excluded
- Zero unbound water remaining in the paper sheet model.

Initial and boundary conditions

Initially, the fibres are saturated with water and the pore structure of the paper sheet contains air. The boundary conditions of the 2-dimensional representation is presented in Fig. (3)

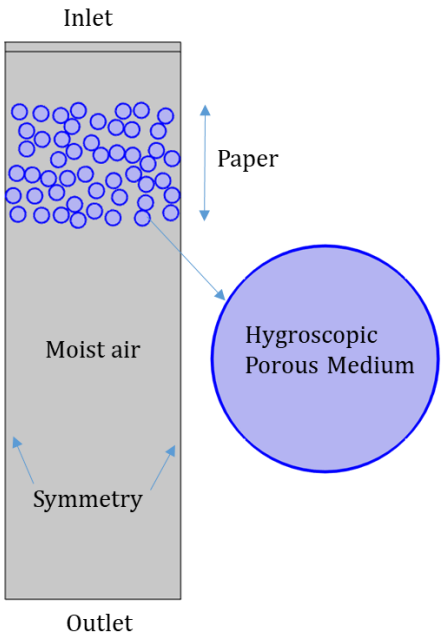

Figure 3. The properties of the computational domain and boundary conditions.

Pressure was applied at the inlet and outlet boundary in which the vacuum level was set at 30 kPa at the outlet and reference pressure at 0 Pa was set at the inlet. Symmetry was set at the vertical boundaries as the fibre structure of the domain which was considered characteristic. Key input parameters for the simulation model are presented in Table (1).

***Table 1**: Key input data to the simulation model*

Parameter data	**Size**
Permeability	$4.8e^{-8}$ [m^2]
Porosity	0.55 [-]
Vapor-air diffusion	$2.6e^{-5}$ [m^2/s]
Vacuum pressure	-30 [kPa]
Density fibre	1340 [kg/m^3]

Mesh setup and solver settings

An unstructured mesh grid containing triangle elements was created for the paper models, see Fig. (4). The grid is solved in a finite element space where a set of basis functions are used to create piecewise linear relations between the mesh elements and convert them to weak formulations for them to be solved. Moreover, geometrical features such as the diameter of a single fibre as well as typical gap distance between adjacent fibres.

A direct linear system solver was used coupled with an implicit second order backward differentiation formula (BDF) solver. The direct solver is called PARDISO which handles sparse linear systems using LU factorization to compute a solution. More information on the solver is found in COMSOL documentation. The BDF solver performs time stepping using a backward differentiation with a maximum order of accuracy of 2, which is the degree of the interpolating polynomial.

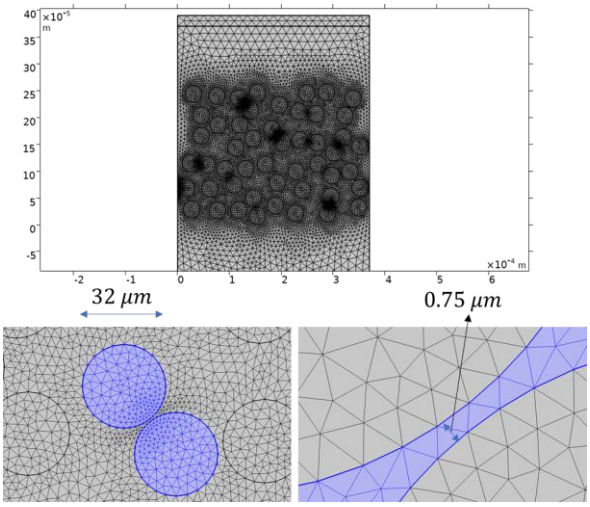

Figure 4. Grid resolution and geometrical properties of the paper sheet model.

Results and Discussion

The results are comprised by presenting the solid content of the fibre web over time. Fig. (5) presents four snapshots of the solid content at times 0, 5, 10 and 20 ms. Local variations of the solid content are observed at 20 ms which is a result of adjacent fibres blocking the airflow and hence, reducing the influence of convective mass transport. Considering that the fibre web is viewed in two dimensions, the air blockage should be overrepresented and thus, causing larger variations of the airflow. This notion is supported in [33] which concluded that flow resistance in the isotropic fibre arrangement in space is lower than the in-plane isotropic orientation and disordered unidirectional fibre arrangements at creeping flow conditions for low to moderate

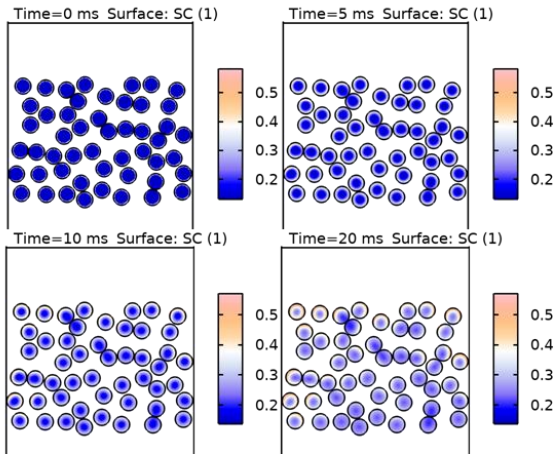

Figure 5. Colour plot representing solid content in in the fibre structure

The averaged solid content for the entire fibre web is presented in Fig. (5)

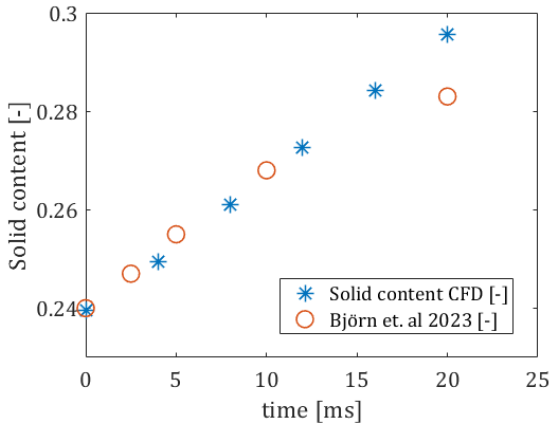

Figure 6. Solid content comparison to laboratory trials performed by [20]

The solid content from the simulation model is compared to lab-scale data from [20], for early TAD molding the simulation model show great coherence with the laboratory results. After some time, the laboratory results deviate from the linear behaviour and display diminishing returns. A few additions need to be added to the models to capture the diminishing returns. In a first approach to establish a numerical model of the TAD molding process, the influence of web deformation was excluded which eliminates both compressibility of the sheet which leads to decreasing permeability and also the rewetting phenomena, which are important factors to consider for a comprehensive model [39, 40]. The TAD fabric is likewise excluded from the simulations. According to [12] machine clothing such as forming fabrics affects the dewatering rate and magnitude through three main parameters, fabric caliper, void volume and air permeability. Similar dependence on the process is assumed to be influenced by TAD fabrics. Adding some of these to the numerical models, it is hypothesized to better simulate both laboratory and pilot scale results.

Conclusions

The first draft of the simulation model shows promising results in terms estimating average solid content over dwell time. At least that is the case up until roughly 15 ms. Based in laboratory results, the solid content rate seems to converge to an upper limit value, which is not the case for the simulation model. Hence, experiments indicate that there is a physical limit on the dewatering rate. The surface moisture vaporization needs to by analysed further as theory suggest that there should be an increased resistance to surface vaporization as the moisture level decreases in the porous media. However, since the dryness levels during the TAD molding process ranges about 5-6% from start to finish, it should have a neglectable affect as there is still a lot of bound water in the fibre. Other limiting factors that are not considered at the moment are:

- Including the TAD wire which add blockage to the airflow as well as absorbs water from the fibres
- Analysing the TAD molding process in a 3-dimensional space which should have an overall reduction in blockage due to an added dimension where the flow can travel.
- Including the deformation of the fibre web during the molding process. Perhaps the poroelastic physics interface could be utilized to analyse both the deformation of the fibre web as the fluid transport of the porous media simultaneously.

Acknowledgements

The authors are grateful for the financial support of the Knowledge foundation, Grant No. 2022-0024, as well as generous in-kind contributions from Albany International Inc., Karlstad University and Valmet AB.

References

[1] Hubbe MA, Sjostrand B, Nilsson L, Koponen A, McDonald JD. Rate-limiting Mechanisms of Water Removal during the Formation, Vacuum Dewatering, and Wet-pressing of Paper Webs: A Review. Bioresources. 15(4) (2020) 9672-755,

[2] Ramaswamy S. Vacuum dewatering during paper manufacturing. Dry Technol. 21(4) (2003) 685-717, https://doi.org/10.1081/Drt-120019058

[3] Attwood BW. A study of vacuum box operation. Paper Technology. 3(5) (1962) T144-T53,

[4] Neun JA. Performance of High-Vacuum Dewatering Elements in the Forming Section. Tappi J. 77(9) (1994) 133-8,

[5] Neun JA. High-vacuum dewatering of newsprint. Tappi J. 79(9) (1996) 153-7,

[6] Räisänen K, Karrila, S., Maijala, A. Vacuum dewatering optimization with different furnishes. Pap Puu-Pap Tim. 78(8) (1996) 455-,
[7] Baldwin L. High vacuum dewatering. Paper Technology. 38(4) (1997) 23-8,
[8] Räisänen KO. Vacuum systems. In: Gullichsen HPJ, editor. Papermaking part 1: Stock preparation and wet end 2000. p. 417-30.
[9] Sjöstrand B. Vacuum Dewatering of Cellulosic Materials: Karlstad University; 2020.
[10] Wahlstrom B. Wet pressing in the 20th century: Evolution, understanding and future. Pulp Pap-Canada. 102(12) (2001) 81-8,
[11] Kuhasalo A, Niskanen, J., Paltakari, J., Karlsson, M. Introduction to paper drying and principles and structure of a dryer section. In: Gullichsen PJ, editor. Papermaking part 2, Drying 2000. p. 16-53.
[12] Granevald R, Nilsson LS, Stenstrom S. Impact of different forming fabric parameters on sheet solids content during vacuum dewatering. Nord Pulp Pap Res J. 19(4) (2004) 428-33, https://doi.org/DOI 10.3183/npprj-2004-19-04-p428-433
[13] Pujara J, Siddiqui MA, Liu Z, Bjegovic P, Takagaki SS, Li PY, et al. Method to characterize the air flow and water removal characteristics during vacuum dewatering. Part I - Experimental method. Dry Technol. 26(3) (2008) 334-40, https://doi.org/10.1080/07373930801898091
[14] Aslund P, Vomhoff H. Method for studying the deformation of a fibre web during a suction pulse. Nord Pulp Pap Res J. 23(4) (2008) 398-402, https://doi.org/DOI 10.3183/npprj-2008-23-04-p398-402
[15] Sjöstrand B, Barbier, C., & Nilsson, L. . Influence on sheet dewatering by structural differences in forming fabrics. Paper Conference and Trade Show Cincinnati, Ohio, USA2016. p. 767-76.
[16] Sjostrand B, Barbier C, Nilsson L. Modeling the influence of forming fabric structure on vacuum box dewatering. Tappi J. 16(8) (2017) 477-83, https://doi.org/Doi 10.32964/Tj16.8.477
[17] Sjostrand B, Barbier C, Ullsten H, Nilsson L. Dewatering of Softwood Kraft Pulp with Additives of Microfibrillated Cellulose and Dialcohol Cellulose. Bioresources. 14(3) (2019) 6370-83, https://doi.org/10.15376/biores.14.3.6370-6383
[18] Rahman H, Engstrand P, Sandstrom P, Sjostrand B. Dewatering properties of low grammage handsheets of softwood kraft pulps modified to minimize the need for refining. Nord Pulp Pap Res J. 33(3) (2018) 397-403, https://doi.org/10.1515/npprj-2018-3037
[19] Sjostrand B, Brolinson A. Addition of Polyvinylamine in Chemi-thermomechanical Pulp and Kraft Pulp and the Effects on Dewatering, Strength, and Air Permeance. Bioresources. 17(3) (2022) 4098-115, https://doi.org/10.15376/biores.17.3.4098-4115
[20] Sjostrand B, Danielsson M, Lestelius M. Method for Studying Water Removal and Air Penetration during Through Air Drying of Tissue in Laboratory Scale. Bioresources. 18(2) (2023) 3073-88, https://doi.org/10.15376/biores.18.2.3073-3088
[21] Sjostrand B. Progression of Vacuum Level in Successive Vacuum Suction Boxes in a Paper Machine-Impact on Dewatering Efficiency and Energy Demand-A Laboratory Study. Bioresources. 18(2) (2023) 3642-53, https://doi.org/10.15376/biores.18.2.3642-3653
[22] Britt KW, Unbehend JE. Water Removal during Paper Formation. Tappi J. 68(4) (1985) 104-7,
[23] Granevald R. Vacuum dewatering of low-grammage paper webs and fabrics.: Karlstad University; 2005.
[24] Aslund P, Vomhoff H, Waljanson A. The deformation of chemical and mechanical pulp webs during suction box dewatering. Nord Pulp Pap Res J. 23(4) (2008) 403-8, https://doi.org/DOI 10.3183/npprj-2008-23-04-p403-408
[25] Pujara J, Siddiqui MA, Liu Z, Bjegovic P, Takagaki SS, Li PY, et al. Method to characterize the air flow and water removal characteristics during vacuum dewatering. Part II - Analysis and characterization. Dry Technol. 26(3) (2008) 341-8, https://doi.org/10.1080/07373930801898125
[26] Jackson GW, James DF. The Permeability of Fibrous Porous-Media. Can J Chem Eng. 64(3) (1986) 364-74, https://doi.org/DOI 10.1002/cjce.5450640302
[27] Zhu S, Pelton RH, Collver K. Mechanistic Modeling of Fluid Permeation through Compressible Fiber Beds. Chem Eng Sci. 50(22) (1995) 3557-72, https://doi.org/Doi 10.1016/0009-2509(95)00205-J
[28] Nilsson L, Stenstrom S. A study of the permeability of pulp and paper. Int J Multiphas Flow. 23(1) (1997) 131-53, https://doi.org/Doi 10.1016/S0301-9322(96)00064-X
[29] Matthews GP. Computer modelling of fluid permeation in porous coatings and paper - an overview. Nord Pulp Pap Res J. 15(5) (2000) 476-85, https://doi.org/DOI 10.3183/npprj-2000-15-05-p476-485
[30] Nilsson L. Stepwise Development of a Mathematical Model for Air Flow in Vacuum Dewatering of Paper. Dry Technol. 32(13) (2014) 1587-97, https://doi.org/10.1080/07373937.2014.909844
[31] Rezk K, Nilsson L, Forsberg J, Berghel J. Modelling of water removal during a paper vacuum dewatering process using a Level-Set method. Chem Eng Sci. 101 (2013) 543-53, https://doi.org/10.1016/j.ces.2013.07.005
[32] Rezk K, Nilsson L, Forsberg J, Berghel J. Simulation of Water Removal in Paper Based on a 2D Level-Set Model Coupled with Volume Forces Representing Fluid Resistance in 3D Fiber Distribution. Dry Technol. 33(5) (2015) 605-15, https://doi.org/10.1080/07373937.2014.967401

[33] Rezk K, Forsberg J, Nilsson L, Berghel J. Characterizing flow resistance in 3-dimensional disordered fibrous structures based on Forchheimer coefficients for a wide range of Reynolds numbers. Appl Math Model. 40(21-22) (2016) 8898-911, https://doi.org/10.1016/j.apm.2016.05.036
[34] Yazdchi K, Luding S. Towards unified drag laws for inertial flow through fibrous materials. Chem Eng J. 207 (2012) 35-48, https://doi.org/10.1016/j.cej.2012.06.140
[35] Koch DL, Ladd AJC. Moderate Reynolds number flows through periodic and random arrays of aligned cylinders. J Fluid Mech. 349 (1997) 31-66, https://doi.org/Doi 10.1017/S002211209700671x
[36] Yazdchi K, Srivastava S, Luding S. Microstructural effects on the permeability of periodic fibrous porous media. Int J Multiphas Flow. 37(8) (2011) 956-66, https://doi.org/10.1016/j.ijmultiphaseflow.2011.05.003
[37] Yazdchi K, Srivastava S, Luding S. Micro-macro relations for flow through random arrays of cylinders. Compos Part a-Appl S. 43(11) (2012) 2007-20, https://doi.org/10.1016/j.compositesa.2012.07.020
[38] Datta AK. Porous media approaches to studying simultaneous heat and mass transfer in food processes. II: Property data and representative results. J Food Eng. 80(1) (2007) 96-110, https://doi.org/10.1016/j.jfoodeng.2006.05.012
[39] Mcdonald JD, Kerekes RJ. Estimating limits of wet pressing on paper machines. Tappi J. 16(2) (2017) 81-7, https://doi.org/Doi 10.32964/Tj16.2.81
[40] Sjostrand B, Barbier C, Nilsson L. Rewetting after high vacuum suction boxes in a pilot paper machine. Nord Pulp Pap Res J. 30(4) (2015) 667-72, https://doi.org/DOI 10.3183/npprj-2015-30-04-p667-672